Surface energetics and thermal roughening of Ag(115) studied with STM movies

M. S. Hoogeman, D. C. Schlößer,* J. B. Sanders, L. Kuipers,† and J. W. M. Frenken
FOM–Institute for Atomic and Molecular Physics, Kruislaan 407, 1098 SJ Amsterdam, The Netherlands
(Received 1 February 1996)

We present a high-speed scanning tunneling microscope (STM) study of the energetics and the thermal roughening transition of the Ag(115) surface. Using a statistical analysis of large numbers of STM images we directly determine the kink creation energy and the step interaction energy. From these two energies we predict the roughening temperature after the terrace-ledge-kink model of Villain *et al.* This prediction is compared with an experimental estimate of the roughening temperature, obtained from STM observations at elevated temperatures. In addition, we derive an interaction energy for two neighboring kinks.
[S0163-1829(96)50220-1]

Atomic-scale properties of crystal surfaces, such as step and kink creation energies, step interaction energies, adatom/vacancy creation energies, and activation energies for diffusion are the fundamental parameters in many surface processes, for example, surface phase transitions and growth phenomena.[1,2] In principle, the scanning tunneling microscope (STM) can be used to address these properties on a quantitative level.[3–7] However, since the STM is intrinsically a slow instrument, the energies are usually derived either *indirectly*, from, e.g., step distance distributions and step fluctuations, or directly, by counting specific local geometries in surface configurations that are *quenched* from a temperature well above the observation temperature. Obviously, both approaches have their disadvantages. In this paper we present the first *direct* STM measurement under *equilibrium* conditions of two energy parameters of a metal surface: the kink creation energy, W_0, and a step interaction energy, w_2. The energy measurements were performed on the Ag(115) surface at room temperature. At this temperature Ag(115) shows such a high surface mobility that the surface is always in local thermodynamic equilibrium. We have recorded real-time STM movies (3–5 frames/s)[8] to collect thousands of different snapshot images on local areas which allowed us to perform a detailed statistical analysis. We further used the STM to estimate the roughening temperature T_R of the metal surface. With this estimate of T_R and the measured kink creation and step interaction energies we tested the Terrace-Ledge-Kink (TLK) model for the roughening of vicinal surfaces.[9]

Ag(115) is a stepped surface consisting of (001) terraces with a width of 2.5 atomic spacings, separated by monoatomic steps, denoted as ''primary steps.'' Height differences on this surface are induced by the narrowing or broadening of the (001) terraces. Such irregularities are the result of thermally excited excursions or of local miscuts with respect to the (115) orientation (Fig. 1). Thermally excited excursions are responsible for the roughening transition of this surface at elevated temperatures. Within the TLK model the surface has to pay two prices for an excursion: over the length of the excursion the step distances change, which increases the total step interaction energy and, as each excursion involves two kinks, two times the kink creation energy has to be paid. The surface accommodates local misorientations by creating steps in the (115) terraces, which we denote as ''secondary steps.'' A secondary step parallel to the [110] azimuth results in one broadened or narrowed (001) terrace (Fig. 1). A secondary step along [552] results in an array of adjacent kinks. The secondary steps make it possible to measure the kink creation energy and the step interaction energy directly.

The experiments were performed with a high-speed, high-temperature STM under ultrahigh vacuum conditions ($p < 2\times10^{-10}$ mbar).[10] The STM data presented in this report were obtained with tunneling currents in the range of 0.05 to 0.3 nA and bias voltages in the range of +150 to +250 mV.

The first of the two parameters of interest is the kink creation energy W_0. We determined this energy directly from the spontaneous creation of excursions at secondary steps along [110]. From Fig. 1 it is clear that an excursion at such a secondary step does not involve any change in the total step interaction energy. Thus, the density of such excursions depends only on the kink creation probability, $p = 2e^{-W_0/k_BT}/1+2e^{-W_0/k_BT}$. From the observed kink density $p=(1.9\pm0.1)\times10^{-2}$ we derive a *first* estimate for W_0 of 1360 K (117 meV).

In Fig. 2 we plotted the length distribution of the excursions measured at a secondary step over a length of 108 atomic spacings. Only configurations with equal numbers of left and right kinks were counted in order to avoid the effect of ''forced'' kinks. The solid curve is the excursion length distribution calculated under this restriction for $W_0 = 1350$ K. For excursions shorter than 10 atomic spacings the experimental data deviate strongly from the solid line. We appear to undercount short excursions with the STM. This is a direct consequence of the high mobility and the short lifetime of the shortest excursions compared with the STM imaging time.

We corrected for this effect by counting excursions only if they were at least 11 atomic spacings long. The result is shown in Fig. 3 as a kink-to-kink distance distribution (inset). The curves in Fig. 3 are the distributions expected for different values of W_0. Due to the cut-off at 11 spacings these distributions could not be calculated analytically, but were obtained using a simple Monte Carlo (MC) calculation. In this calculation secondary steps were generated, where p was the kink creation probability per lattice site along the

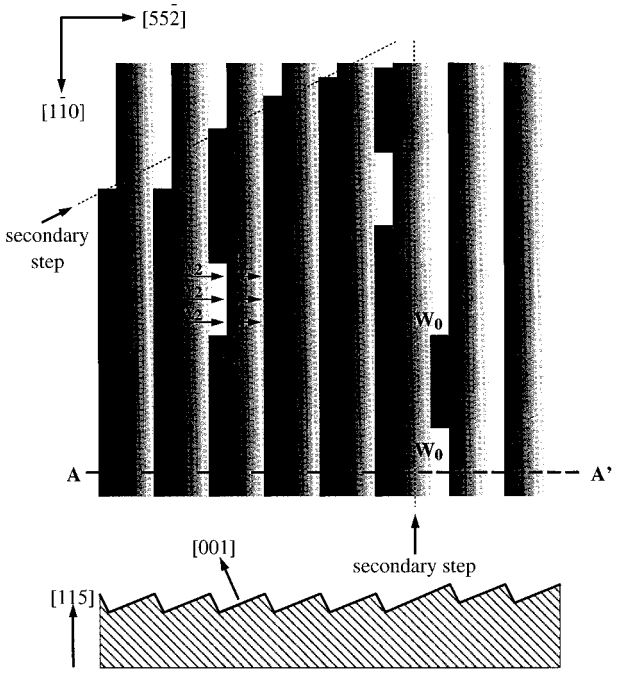

FIG. 1. Schematic representation of the Ag(115) surface. The top view contains eight primary steps. The gray levels represent a height scale. Two secondary steps, induced by a local misorientation, are depicted. One runs along the [110] direction while the other has a [552] component and consists of an array of kinks. The left thermally excited excursion involves both w_2 and W_0, while the two excursions in the secondary step only involve W_0.

step. The kinks were created in both possible directions. From both the experimental secondary steps and the computer-generated step configurations we measured the kink-to-kink distance distribution in a window of 60 atomic spacings. In order to avoid the contribution of forced kinks, only those windows were accepted in which the numbers of left and right kinks were equal.

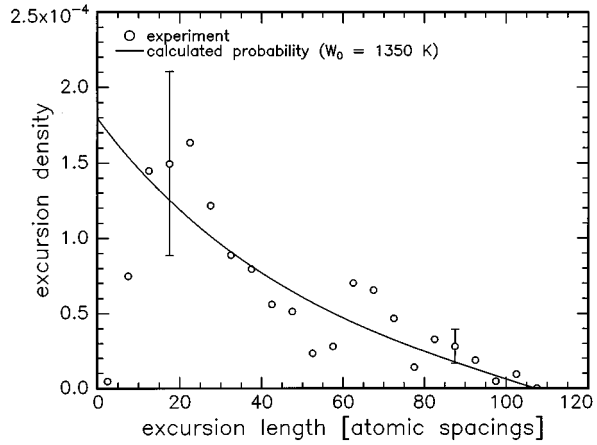

FIG. 2. Excursion length distribution measured at room temperature with a speed of 5 images/s at a [110] secondary step over a length of 108 atomic spacings, obtained from 867 STM images (Ref. 8). The circles are the experimental data and the solid curve represents the calculated density for $W_0 = 1350$ K.

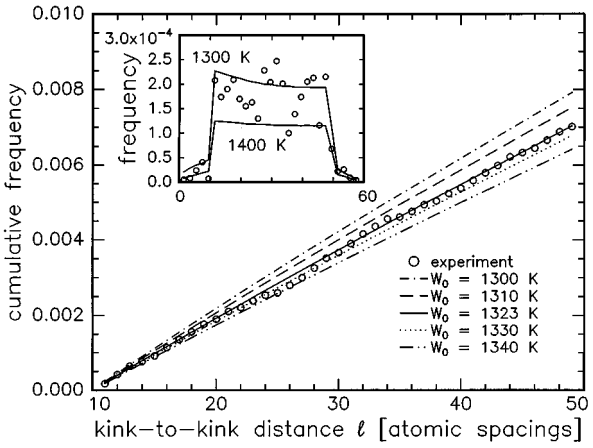

FIG. 3. The cumulative kink-to-kink distance distribution measured for step sections of 60 atomic spacings. The curves are the result of Monte Carlo simulations. Excursions shorter than 11 atomic spacings have been ignored. The inset shows the experimental kink-to-kink distance distribution and Monte Carlo results for W_0=1300 K and W_0=1400 K.

From the inset of Fig. 3 we estimate a W_0 of 1330 ± 50 K (= 117 ± 4 meV). An even more precise value is obtained by comparing the cumulative frequencies of the MC calculations and the experimental data for kink distances between $l = 11$ and $l = 49$ (Fig. 3). From this we *finally* arrive at $W_0 = 1323 \pm 10$ K (= 114 ± 1 meV), where the error bar reflects the statistical uncertainty.

The step interaction energy parameter w_2 is defined as the change in energy per unit length when a primary step shifts by one row of atoms towards one of its neighboring steps. The displaced step has adjacent terraces with widths of 1.5 and 3.5 atomic spacings. In order to measure w_2 we monitored the positions of neighboring forced kinks in secondary steps running close to the [552] direction. In Fig. 4 we focus on three neighboring kinks that belong to a sequence of kinks in such a secondary step. The dashed regions in (a) indicate over which length the primary steps are closer to each other than the regular (115) spacing. As long as the middle kink is positioned between the two outer kinks this length remains constant. Only when the middle kink is outside the region between its two neighbors [Fig. 4(b)] will there be an increase in interaction energy, which is precisely

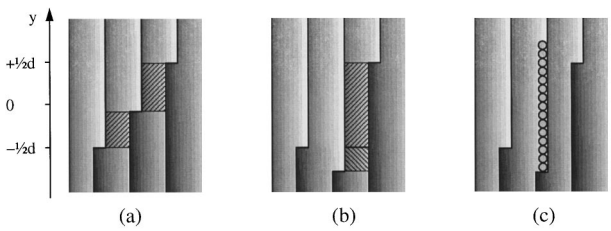

FIG. 4. Schematic representation of a sequence of three neighboring kinks in a secondary step. The dashed regions are the lengths over which the steps are closer to each other than the regular (115) spacing. In (a) the middle kink is between the two outer kinks. In (b) the middle kink is lower than the left kink, which yields an extra change in interaction energy. The kink displacement involves addition or removal of atoms (c).

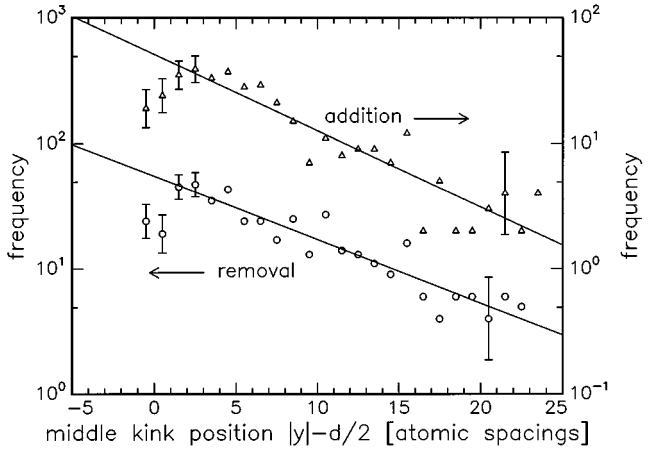

FIG. 5. Semilogarithmic plot of the position distribution of the middle kink for addition or removal of atoms, obtained from 897 STM images, measured at room temperature with a speed of 3 images/s at a [552] secondary step (Ref. 8). The straight lines are fits to the data for $|y|-\frac{1}{2}d>3$ atomic spacings with $w_2 = 35$ K (removal) and $w_2 = 42$ K (addition). The reduced frequencies for $|y|-\frac{1}{2}d=\pm\frac{1}{2}$ atomic spacing indicate a repulsive interaction between kinks in neighboring steps.

w_2 times the length between the middle kink and the nearest outer kink. The expected probability of finding the middle kink at a position y is proportional to the Boltzmann weight:

$$f(y)\propto\begin{cases}1 & |y|<+\frac{1}{2}d\\ e^{-w_2(|y|-\frac{1}{2}d)/k_BT} & |y|>+\frac{1}{2}d\end{cases}, \qquad (1)$$

where d denotes the distance between the two outer kinks and the origin of the y axis has been chosen midway between the two outer kinks. A semilogarithmic plot of the position distribution of the middle kink should yield straight lines with slopes of $-w_2/k_BT$ for $y>\frac{1}{2}d$ and $+w_2/k_BT$ for $y<-\frac{1}{2}d$. The distance d is not fixed but varies from image to image and from triplet to triplet. Because we are only interested in the slopes of the straight lines, which are independent of d, we combined all measured triplet configurations by translating the positions of the middle kink over $\pm\frac{1}{2}d$. In Fig. 5 we plotted the experimental position distributions of the middle kink for $y>\frac{1}{2}d$ (removal of atoms) and for $y<-\frac{1}{2}d$ [addition of atoms, Fig. 4(c)]. We find for addition of atoms an interaction energy of $w_2^+=42\pm4$ K ($=3.6\pm0.3$ meV) per atomic spacing and for removal an interaction of $w_2^-=35\pm3$ K ($=3.0\pm0.3$ meV) per atomic spacing. Naively one would expect the two lines to yield the same interaction energy, i.e., $w_2^+=w_2^-$, as they represent situations that are equivalent in terms of step distances. We suggest that compressive stress of the [001] surface or differences in step relaxation destroy the degeneracy between addition and removal of material. For both distributions in Fig. 5 the frequencies for the two lowest positions ($\pm\frac{1}{2}$) are well below the straight line. From the deviation we conclude that there is a strong, short-ranged repulsive interaction of 260 ± 40 K ($=22\pm3$ meV) between kinks in neighboring steps. A similar kink-kink repulsion between kinks in the same step can also lower the density of short-length excursions.

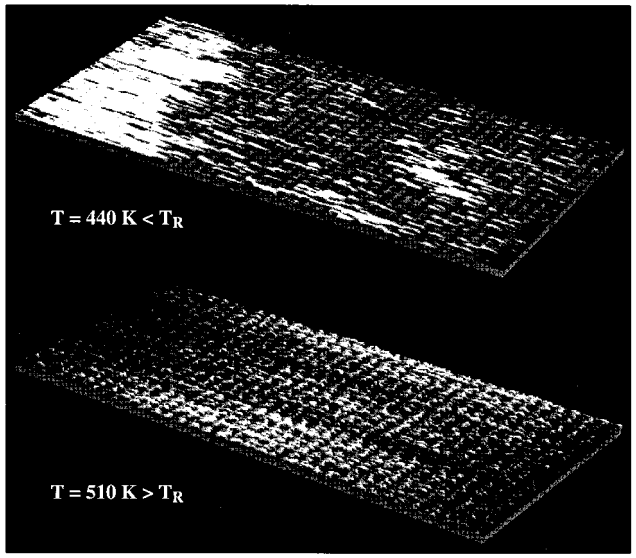

FIG. 6. Perspective representation of two STM images. Below the roughening temperature the secondary step structure is still well resolved (a) (332 Å×165 Å, $V_t = 250$ mV, $I_t = 0.1$ nA, imaging time 5.2 s, $T=440$ K). Above the roughening temperature the secondary step structure is washed out (b) (227 Å×138 Å, $V_t = 250$ mV, $I_t = 0.1$ nA, imaging time 8.8 s, $T=510$ K).

On a vicinal surface T_R is defined as the temperature at which the free energy of a *secondary* step vanishes. This leads to the proliferation of secondary steps, which makes the surface lose its long-range flatness. The spontaneous creation of secondary steps above the roughening temperature washes out the secondary step structure originally present due to local misorientation.[11] This is the most prominent qualitative signature of the roughening transition in STM images. Because it is not possible to make real snapshots with the STM, the time evolution of the surface is interwoven with geometrical information in all STM images. A direct consequence is that step fluctuations in time[12] make the surface look rough already at temperatures below T_R, so that the value of T_R determined with the STM should be regarded as a lower limit, the best estimate coming from the highest-speed measurements. In Fig. 6 we show perspective representations of two STM images at different temperatures. The surface is still below the roughening temperature at 440 K, as the secondary step structure is well resolved. However, the secondary step structure in the image at 510 K appears to be washed out. From these and other STM images we determine a lower limit of the roughening temperature of Ag(115) of 450 K. This value is somewhat higher than that obtained in earlier, slower STM measurements.[13] A quantitative analysis of the roughening transition, based on measured height-height correlation functions, will be reported in a forthcoming publication.

From the measured kink creation energy W_0 and the average step interaction energy $\sqrt{w_2^+w_2^-}$ we can predict the roughening temperature T_R of Ag(115), according to the TLK model:[9,14]

$$\frac{w_2}{k_BT_R}e^{W_0/k_BT_R}=2. \qquad (2)$$

From this equation we numerically determined the value for T_R of 427 ± 10 K. The predicted value is close to the experimental lower limit for T_R of 450 K obtained with the STM. In view of the simplifying assumptions in the TLK model we regard the agreement as excellent. We speculate that the more distant step interactions, which are neglected in the theory, make the (115) surface slightly more stable than the TLK model predicts.

Finally, we compare our experimental results with other experiments and theoretical predictions. From He atom scattering measurements on Cu(115), values of 850 K and 120 K have been derived for W_0 and w_2.[1] W_0 on Ag(115) should be close to the kink energy on Ag(001). The latter energy has been calculated in Refs. 15–17, yielding values of 1180 K, 2470 K, and 950 K, respectively. Najafabadi and Srolovitz[18] have calculated elastic step interaction energies on vicinal fcc-metal surfaces, using the embedded atom method. On the basis of their results we compute a w_2 of 26 K when only dipole interactions are taken into account, but find much smaller or even *negative* values when higher-order correction terms are included.[19] For Cu(115), Hammonds *et al.*[20] predict a w_2 of 62 K, using a Sutton and Chen potential.

In summary, we have used STM movies to accurately determine several energy parameters on a stepped metal surface, Ag(115). We have obtained the kink creation energy $W_0 = 1323 \pm 10$ K and the step interaction energies $w_2^+ = 42 \pm 4$ K and $w_2^- = 35 \pm 3$ K. In addition, we find that nearby kinks in neighboring steps repel each other by 260 ± 40 K. Together with our direct STM observations at elevated temperatures of the roughening transition, the experimental energy values have provided a stringent test of the theory of the roughening of vicinal surfaces.

The authors gratefully acknowledge stimulating discussions with D. Frenkel and H. van Beijeren. We thank R.J.I.M. Koper for the preparation of the Ag sample. This work was part of the research program of the Foundation for Fundamental Research on Matter (FOM), which is financially supported by the Netherlands Organization for Scientific Research (NWO).

---

*Present address: IGV KFA Forschungszentrum Jülich GmbH, D-52425 Jülich, Germany.

†Present address: University of Birmingham, Nanoscale Physics Research Laboratory, Edgbaston, Birmingham, B15 2TT, United Kingdom.

[1] J. Lapujoulade, Surf. Sci. Rep. **20**, 191 (1994), and references therein.

[2] J.A. Venables, G.D.T. Spiller, and M. Hanbücken, Rep. Prog. Phys. **47**, 399 (1984).

[3] E.D. Williams, Surf. Sci. **299-300**, 502 (1994).

[4] L. Masson, L. Barbier, J. Cousty, and B. Salanon, Surf. Sci. **317**, L1115 (1994).

[5] B.S. Swartzentruber, Y.-W. Mo, R. Kariotis, M.G. Lagally, and M.B. Webb, Phys. Rev. Lett. **65**, 1913 (1990).

[6] M. Giesen-Seibert, R. Jentjens, M. Poensgen, and H. Ibach, Phys. Rev. Lett. **71**, 3521 (1994); *ibid.* **73**, 911 (1994).

[7] H.J.W. Zandvliet, H. Wormeester, D.J. Wentink, A. van Silfhout, and H.B. Elswijk, Phys. Rev. Lett. **70**, 2122 (1993).

[8] These movies can be viewed on the World Wide Web at http://www.amolf.nl/external/wwwlab/condensed/surfcrys/index.html

[9] J. Villain, D.R. Grempel, and J. Lapujoulade, J. Phys. F **15**, 809 (1985).

[10] L. Kuipers, R.W.M. Loos, H. Neerings, J. ter Horst, G.J. Ruwiel, A.P. de Jongh, and J.W.M. Frenken, Rev. Sci. Instrum. **66**, 4557 (1995).

[11] J.D. Weeks, in *Ordering in Strongly Fluctuating Condensed Matter Systems*, edited by T. Riste (Plenum, New York, 1980), p. 293, and references therein.

[12] L. Kuipers, M.S. Hoogeman, and J.W.M. Frenken, Phys. Rev. Lett. **71**, 3517 (1993).

[13] J.W.M. Frenken, R.J. Hamers, and J.E. Demuth, J. Vac. Sci. Technol. A **8**, 293 (1990).

[14] W. Selke and A.M. Szpilka, Z. Phys. B **62**, 381 (1986).

[15] R.C. Nelson, T.L. Einstein, and S.V. Khare, Surf. Sci. **295**, 462 (1993).

[16] S.V. Khare and T.L. Einstein, Surf. Sci. **314**, L857 (1994).

[17] P. Stoltze, J. Phys. Condens. Matter **6**, 9495 (1994).

[18] R. Najafabadi and D.J. Srolovitz, Surf. Sci. **317**, 221 (1994).

[19] The results of Ref. 18 actually imply that Ag(115) and other vicinal orientations would be unstable with respect to faceting into (111) and (001) facets.

[20] K.D. Hammonds and R.M. Lynden-Bell, Surf. Sci. **278**, 437 (1992).